

p53 Mutant Human Glioma Cells Are Sensitive to UV-C-Induced Apoptosis Due to Impaired Cyclobutane Pyrimidine Dimer Removal

Luis F.Z. Batista,^{1,2} Wynand P. Roos,² Bernd Kaina,² and Carlos F.M. Menck¹

¹Department of Microbiology, Institute of Biomedical Sciences, University of São Paulo, São Paulo, SP, Brazil and ²Department of Toxicology, University of Mainz, Mainz, Germany

Abstract

The p53 protein is a key regulator of cell responses to DNA damage, and it has been shown that it sensitizes glioma cells to the alkylating agent temozolomide by up-regulating the extrinsic apoptotic pathway, whereas it increases the resistance to chloroethylating agents, such as ACNU and BCNU, probably by enhancing the efficiency of DNA repair. However, because these agents induce a wide variety of distinct DNA lesions, the direct importance of DNA repair is hard to access. Here, it is shown that the induction of photoproducts by UV light (UV-C) significantly induces apoptosis in a p53-mutated glioma background. This is caused by a reduced level of photoproduct repair, resulting in the persistence of DNA lesions in p53-mutated glioma cells. UV-C-induced apoptosis in p53 mutant glioma cells is preceded by strong transcription and replication inhibition due to blockage by unrepaired photolesions. Moreover, the results indicate that UV-C-induced apoptosis of p53 mutant glioma cells is executed through the intrinsic apoptotic pathway, with Bcl-2 degradation and sustained Bax and Bak up-regulation. Collectively, the data indicate that unrepaired DNA lesions induce apoptosis in p53 mutant gliomas despite the resistance of these gliomas to temozolomide, suggesting that efficiency of treatment of p53 mutant gliomas might be higher with agents that induce the formation of DNA lesions whose global genomic repair is dependent on p53. (*Mol Cancer Res* 2009;7(2):237–46)

Introduction

Astrocytic tumors are the most common primary brain malignancies. Among these, glioblastoma is the most malignant

form and has the worst prognosis despite recent advances in surgical and clinical neurooncology (1). Even with extensive treatment involving radical surgery, radiation, and chemotherapy, the median survival time of glioblastoma multiforme (WHO grade IV) is ~1 year from diagnosis (2). Thus, new approaches are required for improving glioma therapy.

The first-line therapy in the treatment of gliomas are alkylating agents, notably temozolomide, which is administered, in recent protocols, concomitant with ionizing radiation (3). Recently, it was shown that temozolomide triggers apoptosis in glioma cells, which is a late response following exposure to this drug (4). It was further shown that the p53 status determines cell killing (5). Thus, human glioma cells with wild-type p53 were extremely sensitive to temozolomide treatment and underwent apoptosis through the extrinsic pathway via FAS receptor activation. In contrast, p53 mutant glioma cells were highly resistant to temozolomide, and the reduced levels of apoptosis observed were due to activation of the intrinsic apoptotic pathway (4).

Because p53 is often mutated in brain tumors, with a frequency of mutation that ranges from 67% in anaplastic astrocytoma to 41% in glioblastoma (6), it is of utmost importance to overcome acquired drug resistance in cells that have p53 inactivation. Within this context, it was recently shown that treatment of glioma cells with the chloroethylating agents ACNU and BCNU induce cell death preferentially in p53 mutant cells (7). That study suggests that p53 mutant cells are more sensitive to ACNU and BCNU treatment due to defective DNA repair. However, because these agents induce several distinct DNA lesions and also DNA-protein cross-links (8), it is difficult to establish the precise role of p53 in the resistance to treatment.

There is a plethora of agents able to induce lesions in the DNA. One of the most frequently studied of these agents is UV-C light. UV-C induces helix-distorting lesions in DNA, such as pyrimidine(6-4)pyrimidone photoproducts and cyclobutane pyrimidine dimers (CPD; ref. 9). The presence of these photolesions in the double-helix produces diverse biological responses in mammalian cells, such as blockage of DNA replication and RNA transcription, chromosomal breakage, DNA recombination, mutations, and, eventually, cell death by apoptosis (10).

In human cells, UV-C-induced DNA lesions are normally removed by nucleotide excision repair (NER). The NER pathway is composed of two subpathways: transcription coupled repair, which removes lesions present in the transcribed strand of actively transcribing genes, and global genomic repair (GGR), which removes lesions from the rest of the genome (11, 12). NER-deficient cells are hypersensitive

Received 9/15/08; revised 10/19/08; accepted 11/3/08; published OnlineFirst 02/10/2009.

Grant support: FAPESP, CNPq, CAPES, and Deutsche Forschungsgemeinschaft DFG KA 724/13-3 and SFB432/B7. C.F.M. Menck is a fellow from the John Simon Guggenheim Memorial Foundation.

The costs of publication of this article were defrayed in part by the payment of page charges. This article must therefore be hereby marked *advertisement* in accordance with 18 U.S.C. Section 1734 solely to indicate this fact.

Note: Present address for L.F.Z. Batista: Department of Medicine, Stanford University School of Medicine, Stanford, CA 94305.

Requests for reprints: Carlos F.M. Menck, Department of Microbiology, Institute of Biomedical Sciences, University of São Paulo, Av. Prof. Lineu Prestes, 1374. Ed. Biomédicas 2, São Paulo, SP 05508-900, Brazil. Phone: 55-11-3091-7499; Fax: 55-11-3091-7354. E-mail: cfmenck@usp.br

Copyright © 2009 American Association for Cancer Research.

doi:10.1158/1541-7786.MCR-08-0428

to UV-C-induced apoptosis (13). Also, removal of photolesions by photolyase was shown to prevent apoptosis (14, 15), indicating that unrepaired DNA lesions are the main cause of UV-C-induced apoptosis in mammalian cells. The role played by p53 on NER has been studied extensively (for a recent review, see ref. 16). p53 accumulates in a dose-dependent manner in cells exposed to UV light through post-transcriptional mechanisms. Over the past few years, it has been shown that p53, or its regulated gene products, contributes to the repair of UV-C-induced DNA damage in human cells, because it regulates the expression of XPC and DDB2, proteins belonging to the GGR pathway of NER (17-19).

The profound effect of p53 on NER regulation and the fact that UV-C is a very effective model to study DNA damage led us to investigate the effects of this DNA-damaging agent in the glioma cell model. Working with p53 wild-type (U87MG) and mutant (U138MG) cells, we show that UV-C light triggers apoptosis in human glioma cells. Interestingly, on UV-C irradiation, p53 mutant cells showed ~10-fold increase in their apoptotic levels, therefore being significantly more sensitive to this agent than p53 wild-type cells. The increased apoptosis in p53 mutant cells correlates with a decreased repair of photo-products. The data also provide evidence that UV-C induces apoptosis in human glioma p53-mutated cells mainly by the intrinsic apoptotic pathway. We propose that DNA-damaging drugs that induce DNA lesions whose repair is dependent on p53, as is the case of bulky lesions, could also trigger this apoptotic pathway in glioma cells, thereby overcoming the resistance of p53 mutant cells toward temozolomide.

Results

Glioma Cells Mutated in p53 Are More Sensitive to UV-C Light-Induced Apoptosis than p53 Wild-type Cells

The apoptotic response to temozolomide and UV-C light was compared in U87MG (p53wt) and U138MG (p53mt; 273Arg-His heterozygous mutation) glioma cells. Analysis of the sub-G₁ population by flow cytometry, a method commonly used for apoptosis quantification, showed that p53 wild-type cells are significantly more sensitive than p53-mutated glioma cells to apoptosis induction by temozolomide (for representative experiment, see Fig. 1A), confirming previous results (4). However, after UV-C irradiation, the opposite effect was observed: p53 wild-type cells were clearly more resistant than p53-mutated cells (Fig. 1A showing data for 30 J/m²). Except for sub-G₁, we did not detect any differences in cell cycle distribution after this dose of UV-C irradiation in the cells tested. Figure 1B shows the time response of induction of apoptosis, showing that U87MG (p53wt) cells were clearly more resistant than U138MG (p53mt) cells for all time points measured. Data also show that apoptosis after UV-C is a late response, occurring >72 h after irradiation of exponentially growing cells. It is important to state that both cell lines have similar doubling times (data not shown).

The sensitivity of p53-mutated cells was further confirmed by colony survival experiments, where U138MG (p53mt) cells were more sensitive than U87MG (p53wt) cells to UV-C (Fig. 1C). To confirm that the relative resistance of U87MG (p53wt) cells is in fact due to p53, the specific p53 inhibitor

pifithrin- α was applied. Pifithrin- α significantly increased the sensitivity of U87MG (p53wt) but not U138MG (p53mt) cells exposed to UV-C, which is in line with a protective role of p53 in UV-C-induced apoptosis. To further substantiate these results, an additional experiment was done, where U87MG (p53wt) cells stably transfected with siRNA targeted to p53 (20) were UV-C irradiated (Fig. 1E). In these cells, p53 was ~75% less expressed than in the parental vector-only transfected cell line (Fig. 1E, *inset*; quantification not shown). The data show that knockdown of p53 in U87MG cells clearly increased the level of apoptosis on UV-C exposure, almost reaching the frequency found in U138MG (p53mt) cells. Also, the role of p53 on the sensibility of glioma cells to UV-C irradiation was further investigated with the use of a different glioma cell pair. Figure 1F shows the results of U343MG (p53wt) and U251MG (p53mt; ²⁷³Arg-His homozygous mutation) cells irradiated with 30 J/m² UV-C. It is clear that U251MG (p53mt) cells are more sensitive to the induction of apoptosis after UV-C when compared with U343MG (p53wt) cells.

To further confirm the data, we analyzed by fluorescence microscopy the amount of apoptotic cells using the terminal deoxynucleotidyl transferase-mediated dUTP nick end labeling (TUNEL) assay. As shown in Fig. 2, U138MG (p53mt) but not U87MG (p53wt) cells displayed after 30 J/m² UV-C irradiation a high extent of DNA fragmentation, which is indicative of apoptosis, supporting the data obtained by sub-G₁ cytometry. Overall, the data show that mutational inactivation or down-regulation of p53 renders human glioma cells sensitive to UV-C light-induced apoptosis.

p53 Is Required for Efficient CPD Removal after UV-C Irradiation in Glioma Cells

The following step was to verify the kinetics of p53 stabilization after UV-C irradiation of human glioma cells. Figure 3A shows a Western blot analysis from nuclear extracts of U87MG (p53wt) and U138MG (p53mt) cells at different times after 30 J/m² UV-C irradiation. p53 stabilizes rapidly in p53 wild-type cells followed by degradation of the protein at later times. We did not detect nuclear p53 in the mutant cell line, although these cells express a mutant form of this protein that is detected in the cytoplasmic fraction without any sort of regulation after UV light (data not shown). The protective effect of p53 against UV-C in glioma cells could be explained by its influence on DNA repair. To substantiate this hypothesis, the amount and persistence of CPDs, the main type of lesion generated by UV-C light (21), was measured in U87MG (p53wt) and U138MG (p53mt) cells as well as in U87MG cells stably transfected with siRNA targeted to p53 (U87sip53) or with an empty vector (U87puro "mock"). As shown in Fig. 3B, UV-C (30 J/m²) induced significant amounts of CPDs in all cell lines tested, which were completely removed 24 h after irradiation in U87MG (p53wt) and U87 "mock"-transfected cells. On the other hand, in U87MG cells transfected with siRNA targeted for p53, there is still a small amount of CPDs after 24 h from irradiation, whereas in U138MG (p53mt) cells these lesions were only partially removed even 24 h after irradiation. Obviously, p53 mutation, or even its down-regulation, causes a slowdown in the rate of repair of CPDs.

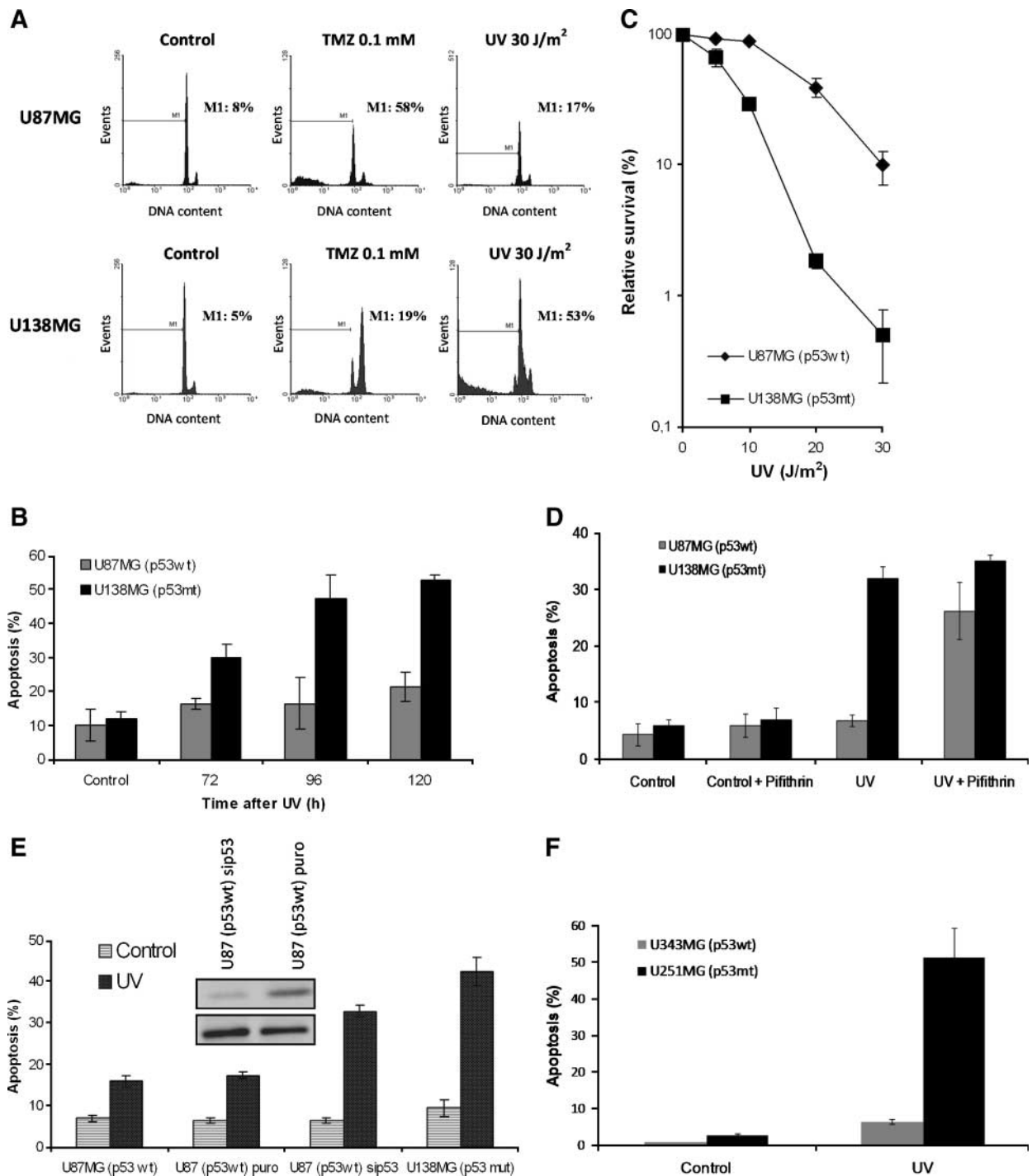


FIGURE 1. Temozolomide and UV light induce apoptosis in U87MG (p53wt) and U138MG (p53mt) human glioma cells. **A.** Analysis of apoptosis after temozolomide or UV light. Approximately 1.0×10^5 U87MG (p53wt) and U138MG (p53mt) cells were treated with temozolomide (0.1 mmol/L) or irradiated with UV light (30 J/m^2) and harvested after 144 h (temozolomide) or 120 h (UV) from treatment. Samples were then analyzed by flow cytometry. The percentage of apoptotic cells (sub-G₁, M₁) is indicated in each histogram. *X* axis, DNA content (relative propidium iodide fluorescence); *Y* axis, cell number (events). **B.** Kinetics of apoptosis after UV light. U87MG (gray columns) and U138MG (black columns) cells were UV irradiated (30 J/m^2), harvested at the indicated times, and analyzed for sub-G₁ content. **C.** Cell survival. U87MG (◆) and U138MG (■) cells were plated at low density, UV irradiated at the indicated doses, and cultivated for 12 d before scoring surviving colonies. **D.** Pifithrin- α sensitizes p53 wild-type cells to UV irradiation. U87MG (gray columns) and U138MG (black columns) cells were irradiated (30 J/m^2), harvested 120 h later, and analyzed for sub-G₁ content. Samples cultivated with pifithrin- α ($30 \mu\text{mol/L}$) were kept with the drug for the entire period after UV irradiation. **E.** p53 inhibition by siRNA in U87MG (p53wt) sensitizes cells to UV irradiation. U87MG (p53wt), U87puro (transfected with an empty vector-mock), U87sip53, transfected with a siRNA sequence targeted to p53, and U138MG (p53mt) cells were irradiated (30 J/m^2), harvested 120 h later, and analyzed for sub-G₁ cells. Inset, Western blot of nuclear p53 in U87sip53 and U87puro ("mock") cells, showing the efficiency of the siRNA targeting. ERK-2 is shown as loading control. **F.** Confirmation of the p53 role with a different pair of glioma cells. U343MG (p53wt) and U251MG (p53mt) cells were irradiated (30 J/m^2), harvested 120 h later, and analyzed for sub-G₁ content by flow cytometry.

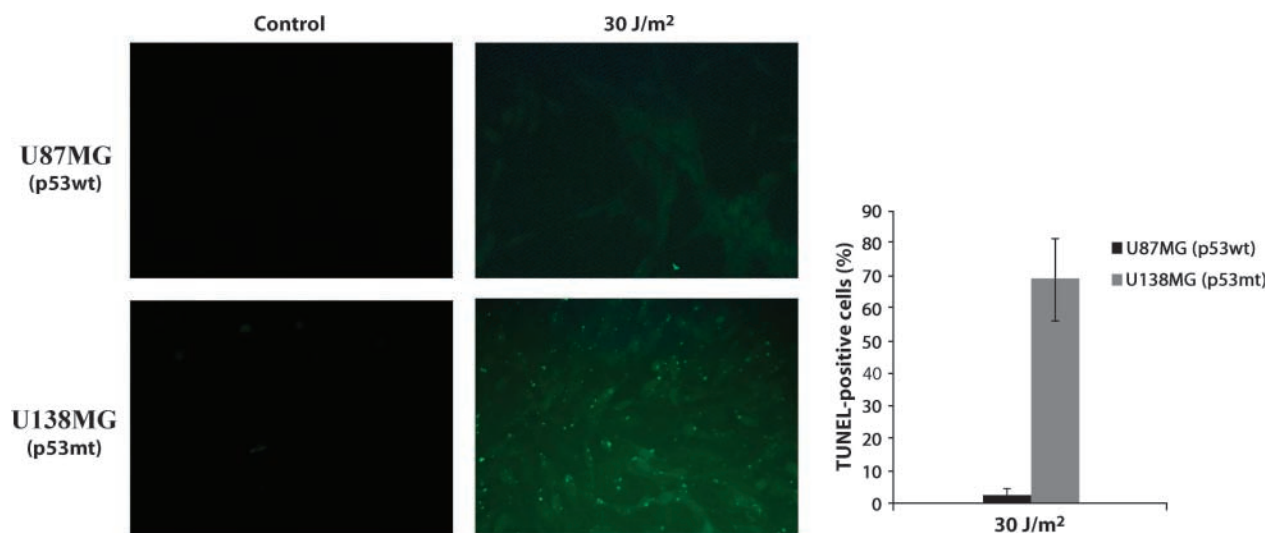


FIGURE 2. UV-induced apoptosis confirmation by the TUNEL assay. U87MG (p53wt) and U138MG (p53mt) were UV irradiated (30 J/m^2) and harvested 96 h later, and apoptosis was analyzed by the TUNEL assay as described in Materials and Methods. Representative images and the correspondent quantification of TUNEL-positive cells in irradiated samples from U87MG (p53wt) and U138MG (p53mt) cells.

UV-C-induced DNA lesions are repaired by the NER pathway. At least two components of this pathway are controlled by p53, that is, XPC and DDB2 (16). Figure 3C shows that these two genes are in fact up-regulated in U87MG (p53wt) but not U138MG (p53mt) cells already 30 min, and up to 8 h, after UV-C irradiation. At the protein level, we also observed a 9-fold increase in XPC levels 24 h after irradiation in U87MG (p53wt) cells, whereas U138MG (p53mt) cells presented only a 1.1-fold increase (data not shown). Thus, the data support the view that the sensitivity of U138MG (p53mt) cells to UV-C light might be due to a decreased efficiency in NER, which is in part controlled by p53.

DNA Replication and RNA Transcription Blockage following UV-C Irradiation of Glioma Cells

CPDs are replication-blocking lesions (9). Therefore, if not repaired, they should reduce the level of DNA synthesis, which would be expected to occur notably in U138MG cells (p53mt), because these cells are impaired in the repair of CPDs (Fig. 3B). To prove this, DNA replication levels after UV-C light exposure of both U87MG (p53wt) and U138MG (p53mt) cells were analyzed. The data shown in Fig. 4A show that DNA synthesis in U87MG (p53wt) and U138MG (p53mt) cells declines steadily until 6 h after UV-C irradiation. Strikingly however, DNA synthesis of U87MG (p53wt) cells starts to recover after this initial period, reaching control levels after 24 h from UV-C irradiation, indicating that replication-blocking lesions were removed from their genome. On the other hand, U138MG (p53mt) cells do not show DNA synthesis recovery. The data are in line with the conclusion that p53-mutated U138MG cells are impaired in NER.

UV-C-induced lesions may also block transcription. Therefore, we investigated the effect of UV-C irradiation on transcription of both cell lines by measuring the incorporation of radiolabeled uridine into RNA. As shown in Fig. 4B, RNA synthesis is attenuated to a higher level in U138MG (p53mt)

than U87MG (p53wt) cells. Similar to DNA synthesis, recovery of transcription did occur in U87MG (p53wt) but not U138MG (p53mt) cells within a 24 h post-incubation period. Evidence is available that both transcription (22) and DNA replication inhibition (23) are involved in triggering apoptosis following UV-C. U138MG (p53mt) cells treated with UV-C under nonproliferating conditions (cells arrested at G₁ phase of the cell cycle by growth without FCS) showed a lower level of apoptosis than proliferating cells (Fig. 4C), which supports the view that UV-C-induced apoptosis of glioma cells is greatly stimulated by proliferation.

p53 Mutant Glioma Cells Undergo Apoptosis following UV-C through Activation of the Intrinsic Death Pathway

Two main pathways for apoptosis have been identified: the death receptor and the mitochondrial damage pathways (24). In both pathways, caspase-3 is the executing caspase. Following UV-C treatment, caspase-3 became activated to a higher level in U138MG (p53mt) than U87MG (p53wt) cells (Fig. 5A), which is in line with the higher apoptosis level observed in U138MG (p53mt) cells. To elucidate which pathway is used by glioma cells following UV-C, cells were UV-C irradiated and post-treated with a FAS receptor antagonizing antibody, therefore blocking the FAS pathway. If any, there was a slight reduction of apoptosis by the anti-FAS antagonizing antibody in U87MG (p53wt) cells irradiated with UV-C light but not at all in U138MG cells (Fig. 5B). For control, similar experiments were done with temozolomide, where a clear reduction of apoptosis of U87MG (p53wt) cells treated with the antibody was observed, confirming previous results (4). To further substantiate this, U87MG (p53wt) and U138MG (p53mt) cells transfected with dominant-negative FADD (DN-FADD) were UV-C irradiated with 30 J/m^2 (Fig. 5C). There was no influence of DN-FADD transfection on the level of apoptosis of UV-C-irradiated U87MG (p53wt) and U138MG (p53mt) cells. The

data suggest that UV-C induces apoptosis in these cells through the mitochondrial damage pathway.

Hallmarks of mitochondrial apoptosis triggered by DNA damage are Bcl-2 decline and increase of Bax and Bak levels (25). Therefore, these proteins were quantified in glioma cells on UV-C exposure. As shown in Fig. 6, there was a clear Bcl-2 decline with a concomitant Bax and Bak up-regulation in U138MG (p53mt) cells irradiated with UV-C light. On the other hand, U87MG (p53wt) cells also showed Bcl-2 decline on UV-C irradiation, but there was no Bax up-regulation. There was no detectable Bak expression in these cells. Therefore, the data are consistent with the conclusion that apoptosis is executed through the intrinsic pathway mediated by the ratio between the antiapoptotic Bcl-2 and the proapoptotic Bax and Bak expression level.

Discussion

Although many chemotherapeutic drugs target DNA, knowledge of the mechanisms of DNA damage triggered cell death in tumor cells is still incomplete. Recently, it was shown that cell death induced by treatment with the methylating agent temozolomide is largely sensitized by wild-type p53, whereas p53 mutant cells are significantly more resistant to this agent (4, 5). This finding immediately implies that glioma treatment with temozolomide might be selecting p53 mutant cells,

resulting in recurrent gliomas, which would be less responsive to the same treatment. In this regard, as p53 is the most common gene altered in cancer (26), any type of treatment that is able to effectively induce apoptosis in a p53 mutant background becomes increasingly important. In this sense, it was also recently shown that treatment of human glioma cells with chloroethylating instead of methylating agents is able to induce apoptosis more efficiently in p53 mutant cells, which was taken to indicate that chloroethylating drugs such as ACNU and BCNU represent a reasonable alternative therapeutic strategy for temozolomide-irresponsible tumors (7). The authors proposed that the higher sensitivity of p53 mutant cells to treatment could be related to defective DNA repair, which was indicated by lack of up-regulation of XPC and DDB2 in p53 mutant glioma cells in response to ACNU (7).

In the present study, data clearly reveal that the generation of CPDs in DNA by UV-C light triggers apoptosis highly efficiently in human p53 mutant glioma cells. The increased sensitivity of p53 mutant cells in comparison with U87MG (p53wt) toward UV-C light is related to a decreased efficiency in the removal of CPDs. The results show that U138MG (p53mt) cells have reduced levels of XPC and DDB2 after UV-C irradiation. This confirms, for the first time in a human glioma model, previous results showing that p53 is a transcriptional activator of these genes following UV-C exposure (17, 18) and that disruption of p53 increases the

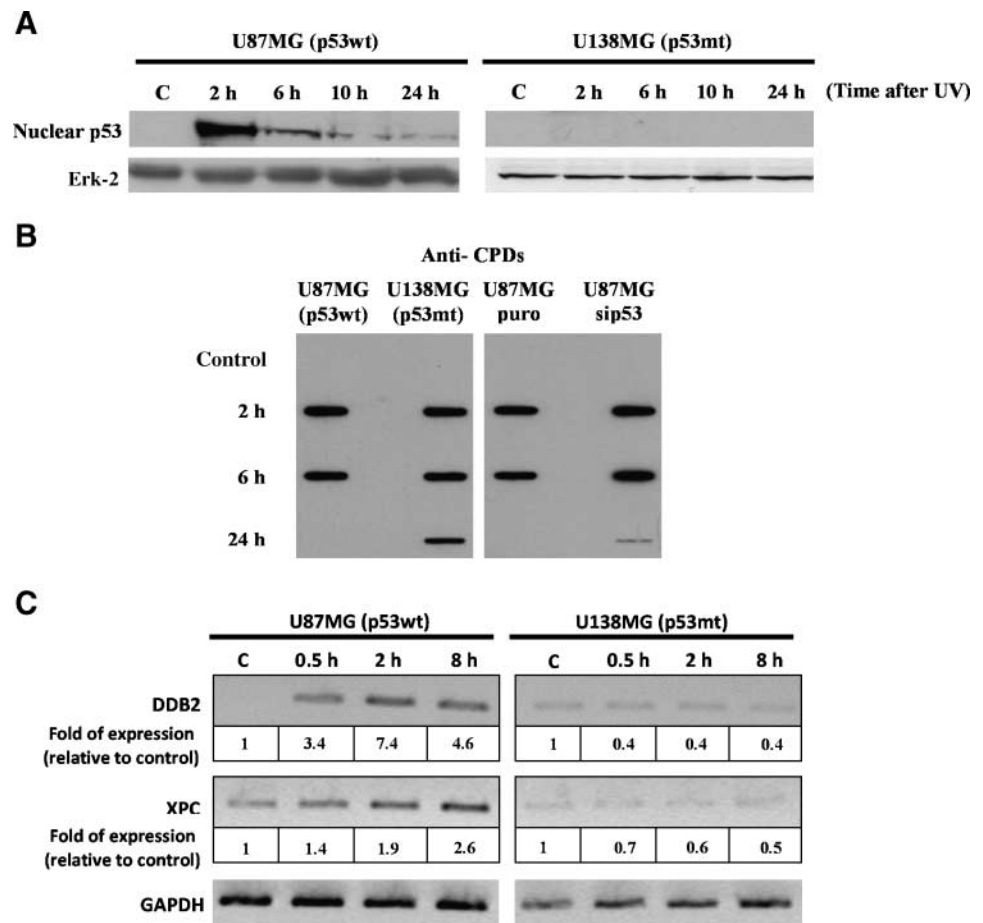


FIGURE 3. Influence of p53 in NER efficiency following UV irradiation. **A.** p53 nuclear localization in U87MG (p53wt) and U138MG (p53mt) at different time points (as indicated) after UV irradiation (30 J/m²). ERK-2 expression is shown as a loading control. **B.** CPD removal different times after UV irradiation (30 J/m²) in U87MG (p53wt), U138MG (p53mt), U87puro, and U87sip53 cells. Different times after UV irradiation (as indicated), genomic DNA was extracted and Southwestern dot-blot analysis was done using an antibody directed against thymine dimers. **C.** XPC and DDB2 expression analysis by reverse transcription-PCR different times after UV irradiation (30 J/m²) in U87MG (p53wt) and U138MG (p53mt) cell lines. The relative fold of expression was done in relation to the expression found in control cells and was calculated after normalization with GAPDH expression in each time point.

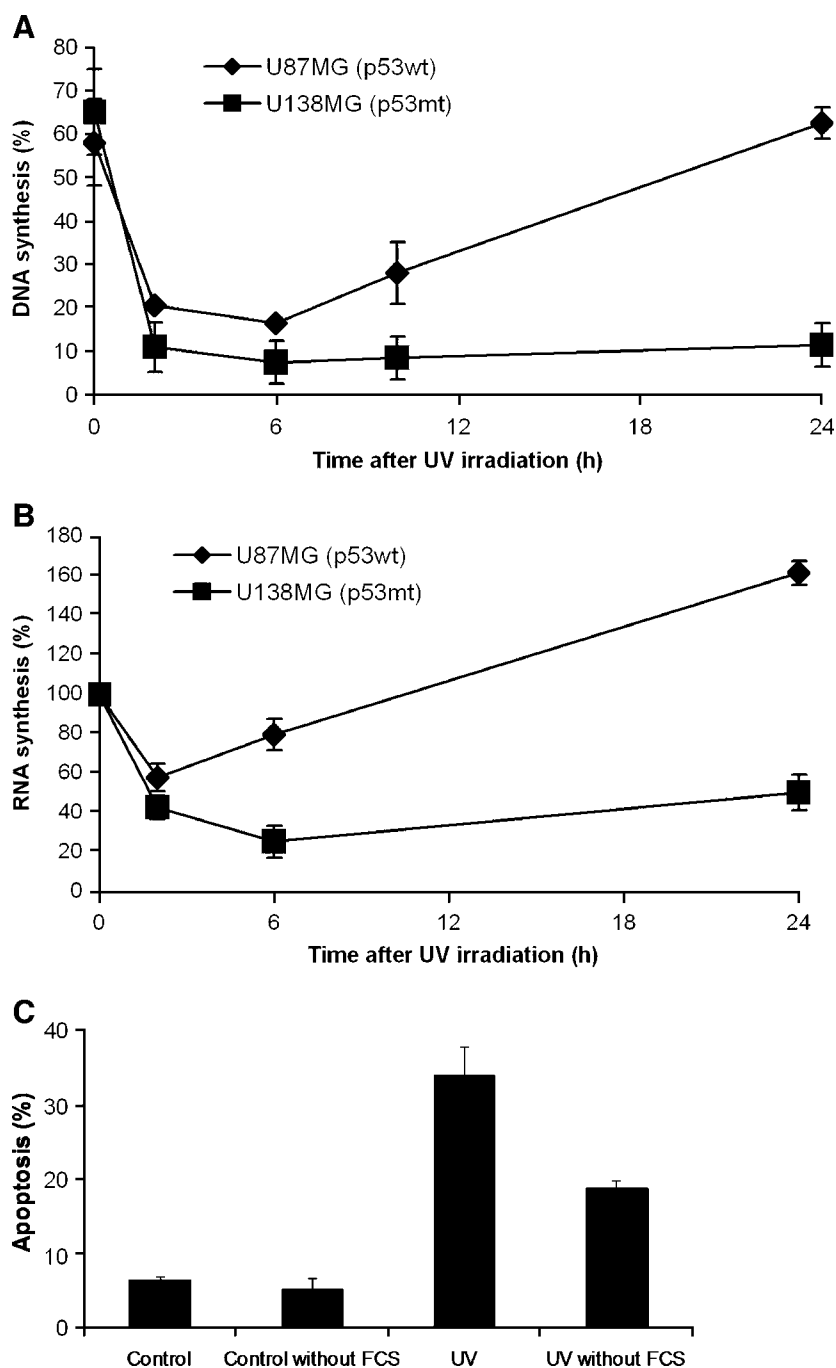


FIGURE 4. Influence of replication blockage and transcription inhibition in UV-induced apoptosis of U87MG (p53wt) and U138MG (p53mt) cells. **A.** Effect of UV irradiation on DNA synthesis of glioma cells. U87MG (◆) and U138MG (■) cells were UV irradiated (30 J/m^2), and different times after irradiation, cells were DNA labeled with [^3H]methylthymidine for 30 min. **B.** Effect of UV irradiation on RNA synthesis of glioma cells. U87MG (◆) and U138MG (■) cells were UV irradiated (30 J/m^2), and different times after irradiation, cells were RNA labeled with [^3H]thymidine for 1 h. DNA and RNA synthesis was determined as described in Materials and Methods. Data are presented in relation to control (nonirradiated) cells. **C.** Apoptosis of U138MG (p53mt) cells is dependent on damaged DNA replication. U138MG cells grown with or without FCS were UV irradiated (30 J/m^2), harvested 120 h after treatment, and analyzed for sub- G_1 content. Samples cultivated in the absence of FCS were maintained in this condition for 48 h before UV irradiation and for the post-treatment incubation time.

sensitivity toward NER-inducing agents (27). In fact, the decreased expression of XPC and DDB2 and p53 deficiency per se seems to impair DNA repair, as CPDs are removed with low efficiency in p53 mutant or down-regulated cells. Because it has been shown that the removal of the other major lesions induced by UV-C, that is, the pyrimidine(6-4)pyrimidone photoproducts, is normally not affected by p53 status of the cell (28), CPDs are most likely the lesions responsible for UV-C-induced apoptosis in this cell model.

It has also been proposed that p53 selectively affects GGR, while having little or no influence on transcription coupled

repair (16), which is in agreement with the increased expression of XPC and DDB2 genes (both active in GGR), in p53 wild-type cells. Thus, the increased UV-C sensitivity of U138MG (p53mt) cells is probably due to a deficiency in GGR, not in transcription coupled repair. It has also been proposed that, in p53 wild-type cells, apoptosis by UV-C light is triggered by the DNA damage-induced blockage of RNA polymerase II (29). Here, we found that p53 mutant cells also present a significantly increased blockage of transcription after UV-C. We also show that these cells are impaired in XPC and DDB2 up-regulation following UV exposure. Because these proteins are not

involved in the repair of transcribed regions of the genome (transcription coupled repair), the results presented here are unable to depict the reason behind the lack of recovery of transcription after UV irradiation in these cells. However, it is tempting to assume that the absence of functional p53 is also related to a decreased transcription coupled repair activity.

On the other hand, DNA replication is also highly inhibited in p53 mutant glioma cells, which is coherent with a decreased GGR activity. Moreover, nonproliferating U138MG (p53mt) cells are significantly more resistant to UV-C-induced apoptosis than proliferating cells. These data support the idea that the blockage of DNA replication by UV-C-induced damage also signals apoptosis. This is in agreement with previous reports, which showed that replication-arrested rodent and human cells do not induce apoptosis following UV-C (30, 31) and that inhibition of DNA synthesis by aphidicolin (an specific inhibitor of replicative DNA polymerases) prevents apoptosis in UV-C-irradiated rodent cells (23). One interesting possibility is that the blockage of replication by CPDs, unrepaired due to the deficiency in GGR, plays a more important role inducing apoptosis in p53 mutant cells than in wild-type glioma cells. Experiments are needed to shed new light on this subject.

Temozolomide- and ACNU-induced DNA lesions were shown to trigger the extrinsic apoptotic pathway in p53 wild-type cells and exclusively the intrinsic pathway in p53 mutant cells (4, 7). The results showed that this is also the case for UV-C-induced DNA lesions, because apoptosis in p53 mutant cells was not inhibited by death receptor pathway neutralization. Also, despite the significant Bcl-2 degradation was observed in both cell lines, only U138MG cells (p53mt) presented a concomitant Bax and Bak up-regulation following UV-C exposure. Because the ratio between these proteins regulates the mitochondrial outer membrane permeabilization (32), the mitochondrial damage pathway appears to be mainly involved in UV-C-induced apoptosis of p53 mutant glioma cells. In fact, it has already been shown that knockdown of p53 accelerates the reduction of antiapoptotic proteins belonging to the mitochondrial pathway of apoptosis, partially mediated by E2F1, increasing the sensitivity to UV light irradiation (33, 34). It is intriguing that although U87MG (p53wt) cells presented Bcl-2 degradation, there was no up-regulation of Bax and Bak. We believe this might be explained by the fast and efficient removal of CPDs from DNA, inhibiting the apoptotic downstream signaling; however, experimental support for this hypothesis is still lacking.

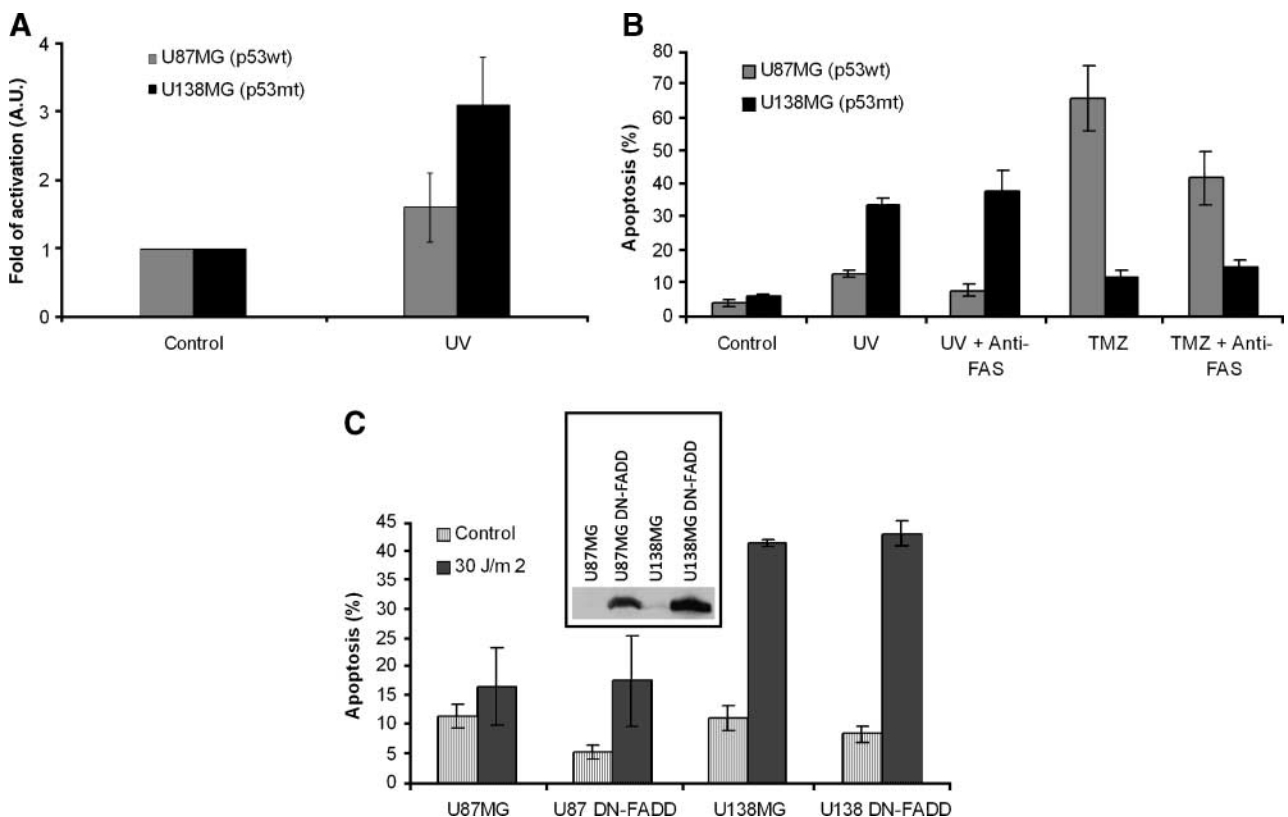


FIGURE 5. Death receptor pathway is not involved in UV-induced apoptosis of human glioma cells. **A.** Caspase-3 activity in UV-irradiated U87MG (p53wt) and U138MG (p53mt) cells. U87MG (gray columns) and U138MG (black columns) cells were UV irradiated (30 J/m²) and 96 h later were collected and had their caspase-3 activity measured with the use of a specific kit (see Materials and Methods). AU, arbitrary units. **B.** Influence of FAS receptor inhibition after UV or temozolomide treatment in U87MG (p53wt) or U138MG (p53mt) cells. U87MG (gray columns) and U138MG (black columns) cells were treated with FAS neutralizing antibody (1 μg/mL) 72 h after UV irradiation (30 J/m²) or temozolomide treatment (0.1 mmol/L). FAS neutralizing antibody was read on the same concentration every 24 h until the nuclei were isolated for apoptosis analysis by sub-G₁ content. **C.** Apoptotic response of U87MG (p53wt), U138MG (p53mt), and the respective DN-FADD clones U87DN-FADD and U138DN-FADD at 120 h after UV irradiation (30 J/m²). Inset, Western blot of FADD expression in the same cell lines, showing efficient clone transfection. Protein loading controls were done.

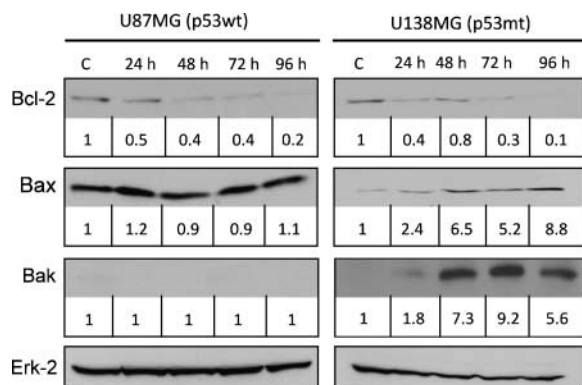


FIGURE 6. Involvement of the intrinsic apoptotic pathway in UV-induced apoptosis of human glioma cells. Western blot analysis of the expression of Bcl-2, Bax, and Bak at different time points (as indicated) after UV irradiation (30 J/m²). ERK-2 is shown as loading control. The densitometric scanning is shown in relation to the expression found in control cells and was calculated after normalization with ERK-2 expression in each time point.

Acquired glioma drug resistance to the current therapy protocols includes the problem that the target tumor cells may be resistant to apoptosis induction and that chemotherapeutic treatment may then lead to the selection of resistant cells, giving rise to tumors that are nonresponsive to the same treatment (35). The understanding of the molecular regulation of apoptosis induction in tumor cells may contribute toward designing strategies for improving current chemotherapeutic protocols during glioma therapy. To this end, we showed that temozolomide-resistant human p53 mutant glioma cells (4) are significantly more sensitive to agents inducing different types of DNA lesion, that is, ACNU-induced lesions (7) and photoproducts generated by UV-C light. Although still theoretical, because the experiments were done under *in vitro* conditions, this work brings important considerations on the mechanisms of acquired tumor resistance to DNA-damaging agents, suggesting that the knowledge of the different DNA repair pathways in specific genetic backgrounds might improve therapy of this devastating disease.

Materials and Methods

Cell Culture

U87MG, U343MG (p53 wild-type), U138MG (273Arg-His heterozygous p53 mutation), and U251MG (273Arg-His homozygous p53 mutation) glioma cell lines (20, 36), the DN-FADD transfectants (U87DN-FADD and U138DN-FADD), and the siRNA (p53)-transfected cells (U87mock and U87sip53) were routinely grown in DMEM (Invitrogen) supplemented with 10% FCS (Cultilab) and 1% antibiotic-antimycotic (Invitrogen) at 37°C in a humidified 5% CO₂ atmosphere.

Transfection of Glioma Cells with DN-FADD and sip53

The transfection method for DN-FADD in human glioma cells has been described in our previous work (4). Briefly, DN-FADD transfectants were generated in U87MG (p53wt) and U138MG (p53mt) cells by transfecting pcDNA3-DN-FADD (37), which contained a *neo* gene for selection. G418-resistant clones were picked in 24-well plates and DN-FADD-positive

clones were determined by Western blotting. siRNA transfectants with siRNA targeted toward p53 were a kind gift of Prof. M. Weller (University of Tubingen) and have already been described before (20).

UV-C Irradiation

Approximately 1.0×10^5 cells were plated in 60 mm Petri dishes 24 h before UV-C irradiation. Cells were washed twice with prewarmed PBS and irradiated by a low-pressure germicidal lamp (UV light emitting mainly at 254 nm, with a dose rate of 1.00 J/m²/s). The UV-C dose was monitored by a VLX 3W radiometer, monochromatic sensor CX-254.

Colony Survival Assay

Approximately 10^3 cells were plated in 60 mm Petri dishes 8 h before UV-C irradiation. Cells were washed twice with prewarmed PBS and irradiated by a low-pressure germicidal lamp (UV light emitting mainly at 254 nm). After irradiation, cells were maintained in complete medium for 10 to 12 days and then fixed with 10% formaldehyde and stained with 1% violet crystal. Survival values were obtained as the ratio of the number of colonies from irradiated cells to nonirradiated cells.

Drug Treatment

Approximately 1.0×10^5 cells were plated in 60 mm Petri dishes 24 h before treatment with different concentrations of temozolomide (Schering-Plough). Temozolomide stocks were prepared by dissolving the drug in DMSO, diluting with sterile H₂O, filtering, and storing at -80°C. The p53 inhibitor pifithrin- α (Calbiochem), which reversibly blocks p53-dependent transcriptional activation (38), was added 1 h before UV-C irradiation and 72 h after treatment with 100 μ M temozolomide. FAS receptor (CD95/Apo1) was inhibited by adding 1 μ g/mL anti-FAS neutralizing antibody (clone ZB4; Biozol Diagnostica Vertrieb) 24 h after UV-C and temozolomide treatments, and every 24 h after the initial treatment, the antibody was readded until samples were harvested. The percentage of population undergoing apoptosis was determined after 120 h for UV-C irradiated samples and after 144 h for temozolomide-treated cells.

Apoptosis Analysis by Flow Cytometry

After different times (indicated for each experiment), both adherent and detached cells were collected and centrifuged at 1,500 rpm for 5 min. Pelleted cells were lysed with 500 μ L of a hypotonic fluorochrome solution (50 μ g/mL propidium iodide in 0.1% sodium citrate + 0.1% Triton X-100) and incubated at least 30 min on ice in the dark. Then, the samples were transferred to microtubes, and propidium iodide fluorescence was measured by flow cytometry (FACSCalibur; Becton Dickinson). Results were obtained as percentage of subdiploid nuclei (WinMDI Software), which represents the apoptotic cells.

Apoptosis Analysis by TUNEL Assay

The Dead End Fluorimetric TUNEL System (Promega) was done according to the manufacturer's protocol. Briefly, cells were plated in Lab-Tek chamber slides (Nalge Nunc), UV-C irradiated or not, and after 96 h post-exposure, cells were fixed

in freshly prepared 4% formaldehyde solution in PBS and permeabilized in 0.2% Triton X-100. The incorporation of fluorescein-12-dUTP(a) at 3'-OH DNA ends using the terminal deoxynucleotidyl transferase recombinant enzyme was carried out for 1 h at 37°C in the dark. Cells were directly visualized by fluorescence microscopy.

Quantification of DNA Synthesis

Approximately 4.0×10^4 cells were plated in 35 mm Petri dishes, and 24 h after plating, cells were UV-C irradiated (30 J/m^2). Different times after UV-C irradiation (indicated on the figure), cells were labeled with [^3H]methyl-thymidine (4.0 mCi/mL; specific activity, 89.0 Ci/mmol; Amersham Pharmacia Biotech) for 30 min. Cells were then washed once with PBS, once with 5% TCA, and twice with hydrated alcohol before 0.3 mol/L NaOH was added. Part of this cell lysate (20% of the total volume) was applied on Whatman 17 paper, which was again washed once with 5% TCA, twice with hydrated ethanol, and once with acetone. Radioactivity was measured with a liquid scintillation spectrometer (Beckman LS 7000). The other part of the lysate (80% of the total volume) was used for absorbance reading at 260 nm (Hitachi U-200 spectrophotometer) for data normalization. The ratio between radioactivity and absorbance expresses the amount of [^3H]methyl-thymidine incorporated by the cells during DNA synthesis.

Quantification of RNA Synthesis

RNA synthesis was determined based on a method described previously (39). Approximately 4.0×10^4 cells were plated in 35 mm Petri dishes, and 24 h after plating, cells were UV-C irradiated (30 J/m^2). Different periods after UV-C irradiation, cells were incubated in a medium containing 3% dialyzed FCS and [^3H]uridine (4.0 mCi/mL; specific activity, 27.0 Ci/mmol; Amersham Pharmacia Biotech) for 30 min. Cells were then harvested and separated into two samples. In one of the samples, cells were lysed [0.3 mol/L NaCl, 20 mmol/L Tris-HCl (pH 8.0), 2 mmol/L EDTA, 1% SDS, and 200 mg/mL proteinase K] and then transferred to Whatman 17 paper and washed twice with 15% TCA and hydrated ethanol for 30 min for radioactivity measurement. The second sample was used to determine the absorbance at 260 nm for data normalization. The ratio between radioactivity and absorbance expresses the RNA synthesis in these cells.

Preparation of RNA and Reverse Transcription-PCR

Total RNA was isolated using the RNA II Isolation Kit (Macherey-Nagel). RNA (2 μg) was transcribed into cDNA by SuperScript II (Invitrogen) in a volume of 40 μL , and 3 μL were subjected to reverse transcription-PCR. Reverse transcription-PCR was done using specific primers (*XPC*: 5'-CTTTGATTTCCATGGCGGCTACTC-3' and 5'-GCTGCTGCTTCTTTCCCTTTT-3' and *DDB2*: 5'-GGGGCTCCAGCAGTCCTTTT-3' and 5'-GGGCCACATGCGTCACTTTCTTT-3'; MWG Biotechnology) and Red-Taq Ready Mix (Sigma).

Dot-Blot Analysis

For dot-blot analysis, both irradiated (30 J/m^2) and nonirradiated U87MG, U138MG, U87mock, and U87sip53 cells were harvested at different times following UV-C

exposure and their genomic DNA was extracted by use of a specific DNA isolation kit (Macherey-Nagel). DNA extraction was done according to the manufacturer's protocol. After DNA quantification by spectrophotometer reading at 260/280 nm, 1.0 μg DNA/sample was loaded into the blotting apparatus and transferred onto polyvinylidene difluoride membranes. Membranes were blocked for 2 h in 5% (w/v) milk powder in PBS containing 0.1% Tween 20, incubated for 2 h with mouse primary antibody (1:1,000 anti-thymine dimers; Kamiya Biomedical), washed three times with PBS-Tween 20, and incubated for 1 h with peroxidase-coupled anti-mouse secondary antibody (1:3,000; Santa Cruz Biotechnology). After final washing with PBS-Tween 20 (three times for 10 min each), blots were developed by using a chemiluminescence detection system (Amersham Pharmacia Biotech).

Preparation of Cell Extracts for Protein Analysis

Treated and untreated cells were harvested by trypsinization, washed once with ice-cold PBS, and resuspended in sonification buffer [20 mmol/L Tris-HCl (pH 8.5), 1 mmol/L EDTA, 5% glycerin, 1 mmol/L DTT, 0.5 mmol/L phenylmethylsulfonyl fluoride]. After sonification, the remaining cell debris was removed by centrifugation at $10,000 \times g$ for 15 min and supernatants were collected.

Western Blot Analysis

Protein (20-30 μg) from cell extracts was separated in a 10% to 12% SDS polyacrylamide gel. Thereafter, proteins were blotted onto a nitrocellulose transfer membrane (Amersham Pharmacia Biotech) for ~ 3 h. Membranes were blocked for 1 h in 5% (w/v) milk powder in PBS, incubated overnight at 4°C with the primary antibody [anti-Bax, anti-Bcl-2, and anti-ERK-2 (Santa Cruz Biotechnology), anti-p53 (Cell Signaling), and anti-Bak (Calbiochem)], washed three times with PBS-Tween 20, and incubated for 1 h with peroxidase-coupled secondary antibody (1:3,000; Sigma). After final washing with PBS-Tween 20 (three times for 10 min each), blots were developed by using an enhanced chemiluminescence detection system (Amersham Pharmacia Biotech).

Caspase-3 Activity Measurement

The caspase colorimetric assay (R&D Systems) was done according to the manufacturer's protocol. Briefly, cells were UV-C irradiated or not, and after 96 h of post-exposure, cells were trypsinized, counted, and collected by centrifugation. Cell pellets were lysed on ice and centrifuged, and the supernatant was transferred and kept on ice. The enzymatic reactions were carried out in 96-well microplates (405 nm, 37°C, 1-2 h) with the addition of an equal volume of $2 \times$ reaction buffer and appropriate caspase colorimetric substrate before the measurement on an ELISA reader.

Disclosure of Potential Conflicts of Interest

No potential conflicts of interest were disclosed.

Acknowledgments

We thank Dr. M. Weller for providing stably p53siRNA-transfected U87MG cells and Dr. Elza Sakamoto-Hojo (University of São Paulo) for the kind gift of U251MG and U343MG cell lines.

References

1. Avgeropoulos NG, Batchelor TT. New treatment strategies for malignant gliomas. *Oncologist* 1999;4:209–24.
2. Sathornsumetee S, Rich JN. New treatment strategies for malignant gliomas. *Expert Rev Anticancer Ther* 2006;6:1087–104.
3. Stupp R, Mason WP, van den Bent MJ, et al. Radiotherapy plus concomitant and adjuvant temozolomide for glioblastoma. *N Engl J Med* 2005;352:987–96.
4. Roos WP, Batista LF, Naumann SC, et al. Apoptosis in malignant glioma cells triggered by the temozolomide-induced DNA lesion *O*⁶-methylguanine. *Oncogene* 2007;26:186–97.
5. Hermisson M, Klumpp A, Wick W, et al. *O*⁶-methylguanine DNA methyltransferase and p53 status predict temozolomide sensitivity in human malignant glioma cells. *J Neurochem* 2006;96:766–76.
6. Fulci G, Ishii N, Van Meir EG. p53 and brain tumors: from gene mutations to gene therapy. *Brain Pathol* 1998;8:599–613.
7. Batista LF, Roos WP, Christmann M, Menck CF, Kaina B. Differential sensitivity of malignant glioma cells to methylating and chloroethylating anticancer drugs: p53 determines the switch by regulating XPC, DDB2, and DNA double-strand breaks. *Cancer Res* 2007;67:11886–95.
8. Scharer OD. DNA interstrand crosslinks: natural and drug-induced DNA adducts that induce unique cellular responses. *ChemBioChem* 2005;6:27–32.
9. Friedberg EC. The eureka enzyme: the discovery of DNA polymerase. *Nat Rev Mol Cell Biol* 2006;7:143–7.
10. Batista LF, Kaina B, Meneghini R, Menck CF. How DNA lesions are turned into powerful killing structures: Insights from UV-induced apoptosis. *Mutat Res* 2008, doi:10.1016/j.mrrev.2008.09.001.
11. Christmann M, Tomicic MT, Roos WP, Kaina B. Mechanisms of human DNA repair: an update. *Toxicology* 2003;193:3–34.
12. Costa RM, Chiganças V, Galhardo Rda S, Carvalho H, Menck CF. The eukaryotic nucleotide excision repair pathway. *Biochimie* 2003;85:1083–99.
13. Dunkern TR, Fritz G, Kaina B. Ultraviolet light-induced DNA damage triggers apoptosis in nucleotide excision repair-deficient cells via Bcl-2 decline and caspase-3/-8 activation. *Oncogene* 2001;20:6026–38.
14. Chiganças V, Batista LF, Brumatti G, Amarante-Mendes GP, Yasui A, Menck CF. Photorepair of RNA polymerase arrest and apoptosis after ultraviolet irradiation in normal and XPB deficient rodent cells. *Cell Death Differ* 2002;9:1099–107.
15. Chiganças V, Miyaji EN, Muotri AR, et al. Photorepair prevents ultraviolet-induced apoptosis in human cells expressing the marsupial photolyase gene. *Cancer Res* 2000;60:2458–63.
16. Ford JM. Regulation of DNA damage recognition and nucleotide excision repair: another role for p53. *Mutat Res* 2005;577:195–202.
17. Adimoolam S, Ford JM. p53 and DNA damage-inducible expression of the xeroderma pigmentosum group C gene. *Proc Natl Acad Sci U S A* 2002;99:12985–90.
18. Hwang BJ, Ford JM, Hanawalt PC, Chu G. Expression of the p48 xeroderma pigmentosum gene is p53-dependent and is involved in global genomic repair. *Proc Natl Acad Sci U S A* 1999;96:424–8.
19. Smith ML, Chen IT, Zhan Q, O'Connor PM, Fornace AJ, Jr. Involvement of the p53 tumor suppressor in repair of U.V.-type DNA damage. *Oncogene* 1995;10:1053–9.
20. Wischhusen J, Naumann U, Ohgaki H, Rastinejad F, Weller M. CP-31398, a novel p53-stabilizing agent, induces p53-dependent and p53-independent glioma cell death. *Oncogene* 2003;22:8233–45.
21. Andressoo JO, Mitchell JR, de Wit J, et al. An Xpd mouse model for the combined xeroderma pigmentosum/Cockayne syndrome exhibiting both cancer predisposition and segmental progeria. *Cancer Cell* 2006;10:121–32.
22. Ljungman M, Zhang F. Blockage of RNA polymerase as a possible trigger for U.V. light-induced apoptosis. *Oncogene* 1996;13:823–31.
23. Batista LF, Chiganças V, Brumatti G, Amarante-Mendes GP, Menck CF. Involvement of DNA replication in ultraviolet-induced apoptosis of mammalian cells. *Apoptosis* 2006;11:1139–48.
24. Adams JM. Ways of dying: multiple pathways to apoptosis. *Genes Dev* 2003;17:2481–95.
25. Chan DC. Mitochondria: dynamic organelles in disease, aging, and development. *Cell* 2006;125:1241–52.
26. Steele RJ, Lane DP. p53 in cancer: a paradigm for modern management of cancer. *Surgeon* 2005;3:197–205.
27. Fan S, Smith ML, Rivet DJ II, et al. Disruption of p53 function sensitizes breast cancer MCF-7 cells to cisplatin and pentoxifylline. *Cancer Res* 1995;55:1649–54.
28. El-Mahdy MA, Hamada FM, Wani MA, Zhu Q, Wani AA. p53-degradation by HPV-16 E6 preferentially affects the removal of cyclobutane pyrimidine dimers from non-transcribed strand and sensitizes mammary epithelial cells to UV-irradiation. *Mutat Res* 2000;459:135–45.
29. Ljungman M, Lane DP. Transcription—guarding the genome by sensing DNA damage. *Nat Rev Cancer* 2004;4:727–37.
30. Dunkern TR, Kaina B. Cell proliferation and DNA breaks are involved in ultraviolet light-induced apoptosis in nucleotide excision repair-deficient Chinese hamster cells. *Mol Biol Cell* 2002;13:348–61.
31. Carvalho H, da Costa RM, Chiganças V, et al. Effect of cell confluence on ultraviolet light apoptotic responses in DNA repair deficient cells. *Mutat Res* 2003;544:159–66.
32. Spierings D, McStay G, Saleh M, et al. Connected to death: the (unexpurgated) mitochondrial pathway of apoptosis. *Science* 2005;310:66–7.
33. Chaturvedi V, Sitailo LA, Qin JZ, et al. Knockdown of p53 levels in human keratinocytes accelerates Mcl-1 and Bcl-x(L) reduction thereby enhancing UV-light induced apoptosis. *Oncogene* 2005;24:5299–312.
34. Knezevic D, Zhang W, Rochette PJ, Brash DE. Bcl-2 is the target of a UV-inducible apoptosis switch and a node for UV signaling. *Proc Natl Acad Sci U S A* 2007;104:11286–91.
35. Steinbach JP, Weller M. Apoptosis in gliomas: molecular mechanisms and therapeutic implications. *J Neurooncol* 2004;70:245–54.
36. Ishii N, Maier D, Merlo A, et al. Frequent co-alterations of TP53, p16/CDKN2A, p14ARF, PTEN tumor suppressor genes in human glioma cell lines. *Brain Pathol* 1999;9:469–79.
37. Tewari M, Dixit VM. Fas- and tumor necrosis factor-induced apoptosis is inhibited by the poxvirus crmA gene product. *J Biol Chem* 1995;270:3255–60.
38. Komarova EA, Gudkov AV. Suppression of p53: a new approach to overcome side effects of antitumor therapy. *Biochemistry (Mosc)* 2000;65:41–8.
39. Balajee AS, May A, Dianov GL, Friedberg EC, Bohr VA. Reduced RNA polymerase II transcription in intact and permeabilized Cockayne syndrome group B cells. *Proc Natl Acad Sci U S A* 1997;94:4306–11.

Molecular Cancer Research

p53 Mutant Human Glioma Cells Are Sensitive to UV-C-Induced Apoptosis Due to Impaired Cyclobutane Pyrimidine Dimer Removal

Luis F.Z. Batista, Wynand P. Roos, Bernd Kaina, et al.

Mol Cancer Res 2009;7:237-246. Published OnlineFirst February 10, 2009.

Updated version Access the most recent version of this article at:
doi:[10.1158/1541-7786.MCR-08-0428](https://doi.org/10.1158/1541-7786.MCR-08-0428)

Cited articles This article cites 38 articles, 12 of which you can access for free at:
<http://mcr.aacrjournals.org/content/7/2/237.full#ref-list-1>

E-mail alerts [Sign up to receive free email-alerts](#) related to this article or journal.

Reprints and Subscriptions To order reprints of this article or to subscribe to the journal, contact the AACR Publications Department at pubs@aacr.org.

Permissions To request permission to re-use all or part of this article, use this link
<http://mcr.aacrjournals.org/content/7/2/237>.
Click on "Request Permissions" which will take you to the Copyright Clearance Center's (CCC) Rightslink site.